Interconvertible geometric isomers of *Plasmodium falciparum* dihydroorotate dehydrogenase inhibitors exhibit multiple binding modes

Glenn A. McConkey[a], Paul T. P. Bedingfield[a], David R. Burrell[b], Nicholas C. Chambers[b], Fraser Cunningham[c], Timothy J. Prior[b], Colin W.G. Fishwick[c], Andrew N. Boa[b*]

[a] *School of Biology, Faculty of Biological Sciences, University of Leeds, Leeds LS2 9JT, UK*

[b] *School of Mathematics & Physical Sciences, Faculty of Science and Engineering, University of Hull, Hull HU6 7RX, UK*

[c] *School of Chemistry, Faculty of Mathematics and Physical Sciences, University of Leeds, Leeds LS2 9JT, UK*

Abstract

Two new tricyclic β-aminoacrylate derivatives (**2e** and **3e**) have been found to be inhibitors of *Plasmodium falciparum* dihydroorotate dehydrogenase (*Pf*DHODH) with Ki 0.037 and 0.15 μM respectively. ^{1}H and ^{13}C NMR spectroscopic data show that these compounds undergo ready *cis-trans* isomerisation at room temperature in polar solvents. *In silico* docking studies indicate that for both molecules there is neither conformation nor double bond configuration which bind preferentially to *Pf*DHODH. This flexibility is favourable for inhibitors of this channel that require extensive positioning to reach their binding site.

Keywords: dihydroorotate dehydrogenase; DHODH; *Plasmodium falciparum*; inhibitor

**Corresponding author*. Tel.: +44 (0)1482 465022; E-mail address: a.n.boa@hull.ac.uk

Malaria is one of the main infectious diseases in the world with an estimated 212 million cases in 2015, centred to a great extent on the countries in central Africa and south east Asia.[1] The numbers are even starker when one considers it is estimated these cases led to an estimated 429,000 deaths and that approximately 70% of these deaths were of children under five years old. Malaria is considered a 'preventable' disease, largely because of the use of chemotherapeutic agents,[2] however widespread drug resistance[3] has rendered these agents ineffective in many regions of the world. This problem has led to much effort being expended into validating novel drug targets, as well as discovering small molecule enzyme inhibitors to act as leads for development of new antimalarial drugs.[4] One such target which has attracted recent attention is *P. falciparum* dihydroorotate dehydrogenase (*Pf*DHODH),[5] a key enzyme in the obligate *de novo* pyrimidine pathway for uridine monophosphate (UMP) biosynthesis. Early work aimed towards the discovery of *Pf*DHODH inhibitors focussed on modification of the human DHODH (*h*DHODH) inhibitors known at the time, such as brequinar (Figure 1).[6] This work was naturally followed by high throughput screening[7] and *de novo* design approaches.[8] During the progress of this work, co-crystallisation[9] and *in silico* docking[8,10] experiments revealed that the inhibitors discovered targeted the ubiquinone binding channel, and also revealed important features for the design of selective and potent inhibitors. Firstly amino acid residues H185 and / or R265, at the head of the ubiquinone-binding channel, were found to be essential for hydrogen bonding interactions with the inhibitors. The ubiquinone channel also contained a hydrophobic region which contributes to the binding of the more potent inhibitors reported. Indeed many of the inhibitors reported to date[6-12] reveal broadly this amphiphilic nature, and possess a polar 'head group' and hydrophobic 'tail'. Triazolopyrimidine DSM265 (Figure 1) is currently the most advanced *Pfal*DHODH inhibitor, and Phase 1 clinical trials for this candidate have recently been reported.[13]

We have reported previously that β-aminoacrylate derivatives of the general structure **1** (Figure 1) are inhibitors of *Pf*DHODH.[10] In particular, tricyclic derivatives **2a** and **3b** displayed sub-micromolar

IC_{50} values against *Pf*DHODH, and in the case of **2a** there was a 1000-fold greater potency compared to the human enzyme (*h*DHODH). An extensive series of experiments in this previous work with this class of inhibitors[10a] showed that compounds **2a** and **3b**, and related structures, were competitive inhibitors with the enzyme cofactor CoQ and reversible. Compounds such as **2a** may in principle exist as a pair of geometric isomers and we considered that different H-bonding groups on either side of the double bond, and their position relative to the aromatic portion of the structure through rotation about the C_{Ar}-N bond, would be key in determining their binding to the enzyme. It is perhaps noteworthy to mention that alternative binding modes have been reported with certain *h*DHODH inhibitors,[14] and also differential binding modes for A77 1726, the active metabolite of leflunomide (Figure 1), when binding to *Pf*DHODH is compared to its principal target *h*DHODH.[9a] We therefore sought to examine whether alterative polar 'head groups' to those investigated would lead to improved activity of members in this class of compound, and the results obtained are reported herein.

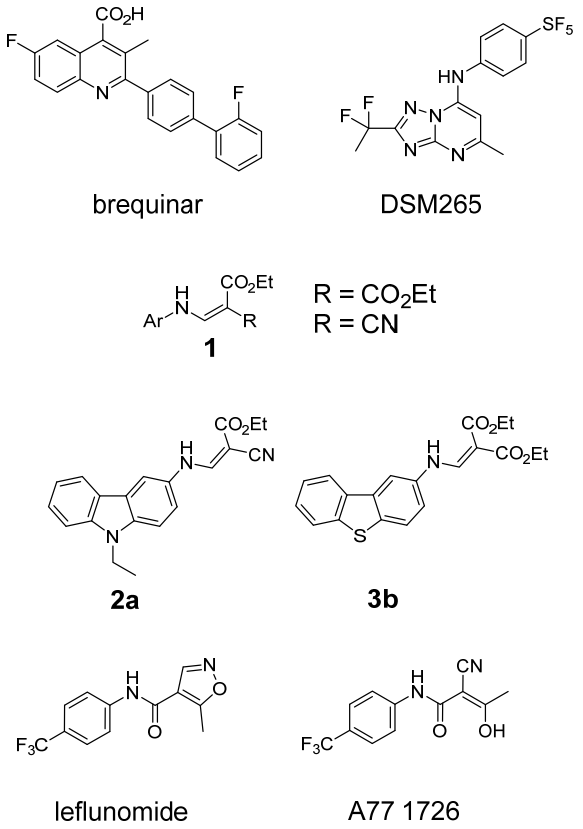

Figure 1. Example structures of known *Pfal*DHODH (brequinar, DSM265, **2a** and **3b**) and *h*DHODH (A77 1726) inhibitors.

Ten new derivatives (**2b-f**, **3a,c-f**) based on the 3-aminocarbazole (**4**) and 3-aminodibenzothiophene (**5**) core unit were synthesised using the method reported previously (Scheme 1).[10a] Derivatives **2b** and **3a** were prepared by simply heating the aromatic amine with the appropriate commercially available β-ethoxy-α,β-unsaturated carbonyl compound **6b** and **6a** respectively. For **2c-f** and **3c-f** the relevant active methylene compounds **7c-f** were first heated with an excess of triethylorthoformate (or acetate) in toluene, forming the β-ethoxy-α,β-unsaturated carbonyl compounds **6c-f** *in situ*, followed by addition of either the aromatic amine **4** or **5** and heating for a further short period. After cooling, the products precipitated upon standing, were collected by filtration and then recrystallised.[15]

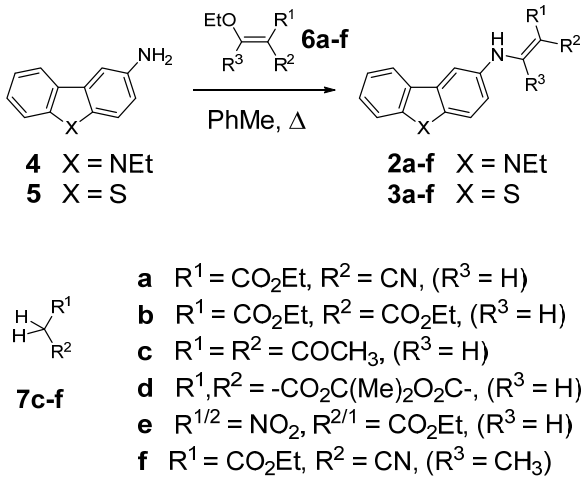

Scheme 1. Synthesis of β-aminoacrylate derivatives of 9-ethyl-3-aminocarbazole and 3-aminodibenzothiophene in this study.

Table 1 shows the IC_{50} values obtained for the compounds discussed in this work. These values were obtained using the screening methodology reported previously.[10a] The IC_{50} values of derivatives **2c,d,f** and **3c,d,f** were above the arbitrary cut-off value of 0.1 mM and thus not further examined. Derivatives **2d** and **3d**, structures based upon Meldrum's acid, are conformationally restricted analogues. We assigned their low activity to the restricted freedom imposed by the six-membered ring to position the polar head group for maximal hydrogen bonding to H-bond donors on either side the co-factor channel.

Entry	*Pfal*DHODH IC_{50} (μM)	hDHODH IC_{50} (μM)
2a	0.28 ± 0.05 0.44 ±0.06 [10a]	491 ± 42 [10a]
3a	1.2	n.d.
2b	4.4	n.d.
3b	0.16 ± 0.05 0.16 ± 0.05 [10a]	30 ± 5.9 [10a]
2c	>100	n.d.
3c	>100	n.d.
2d	>100	n.d.
3d	>100	n.d.
2e	0.094 ± 0.031 †	>100
3e	0.38 ± 0.06 ‡	>100
2f	>100	n.d.
3f	>100	n.d.

Table 1. IC_{50} values of selected compounds against *P. falciparum* and human DHODH. The IC_{50} values were determined according to methodology reported previously.[10a] n.d. = not determined; † Ki vs *Pfal*DHODH) for **2e** was 0.037±0.012 μM; ‡ Ki (*Pfal*DHODH) for **3e** was 0.150±0.001 μM (cf. Ki = 0.05 and 0.02 μM for **2a** and 3**b** respectively[10a])

The activity of the cyanoacetate (**2a**, **3a**) and malonate derivatives (**2b**, **3b**) are not too dissimilar, and the IC_{50} values are probably subtly altered depending on the influence of the second ethyl ester and/or *N*-ethyl group. The lowest activity is seen with **2b**, where both ethyl groups are present, may mean that the molecule is slightly too large to fit well into the ubiquinone binding site. Similarly, derivatives **2f** and **3f**, which only differ from **2a** and **3a** by a single methyl group, showed that substitution at this position cannot be tolerated sterically. The lack of activity in **2c** and **3c** was somewhat surprising, given the similar electron withdrawing effect of the methyl ketone compared to the ethyl ester and cannot so easily be explained.

Nitroacrylate derivatives **2e** and **3e** were as active, if not more so, than cyanoacrylate and malonate derivatives **2a,b** and **3a,b**. As discussed above, we considered that the conformational preferences in the polar 'head group' would be important in determining the binding mode of these inhibitors to DHODH, and so it was interesting in particular to compare the isomerism in carbazole derivatives **2a**, **2e** and **2f**, and the corresponding analogues of the dibenzothiophene series **3a**, **3e** and **3f**. In the case of **2a** and **3a**, evidence of only one isomer is seen in the ^{1}H NMR. The heavily deshielded NH (δ 10.96 ppm for **2a** and 11.26 ppm for **3a**) and large coupling to the -CH= (*J* 13.7 Hz) indicated the presence of intramolecular hydrogen bonding to the ester carbonyl group, and the *anti*-displacement of the hydrogen atoms in the Ar-N*H*-C*H*= unit showed that the (*Z*)-isomer was preferred. In the case of **2f** and **3f** analysis of the products similarly revealed single isomers [δ_{NH} 11.56 (s) for **2f**, and δ_{NH} 11.65 (s) for **3f**] in spite of the extra methyl group (R^3). The nitroacrylate derivatives **2e** and **3e** have the possibility to exhibit intramolecular hydrogen bonding in either isomeric form, and the balance between these isomeric forms was expected to have an important effect on the overall isomeric

preferences and therefore binding to the cofactor channel of DHODH. The ^{1}H NMR of both **2e** and **3e** showed a 1:1 mixture (in $CDCl_3$) however many times it was recrystallised under a range conditions (solvent, rate of cooling etc), indicating no clear preference in solution for one isomer over the other.[16] The ^{13}C NMR of **2e** in $CDCl_3$ showed doubling of almost all signals. However for **3e** in the more polar d_6-DMSO only one set of the aromatic carbon signals and ethyl group were observed, and also the signals for the acrylate unit were completely absent. This was accompanied by changes in the ^{1}H NMR where in d_6-DMSO the NH-CH= signals were broadened significantly and almost reduced to baseline level, and the ethyl CH_2 quartet was greatly broadened. This indicates clearly that the geometric forms of **3e** are readily interconvertible in a polar solvent on the NMR timescale.

Carbazole **2e** could be recrystallised from ethyl acetate to provide bright red crystals suitable for single crystal X-ray diffraction (see Supplementary Information).[17] The first crop showed **2e** had crystallised preferentially as the (*Z*)-isomer (Figure 2A). Examining the single crystal X-ray data of **2e** it was interesting to find that the N2-C15 bond was much shorter than the C15-C16 bond and C9-N2 bonds [1.3201(17) Å vs. 1.3914(18) Å vs. 1.4242(17) Å respectively]. These data are consistent with extensive delocalisation of the nitrogen lone pair into the enamine unit in the (*Z*)-isomer (Figure 2B), and could explain its deep red colour. After evaporation of the mother liquors and another recrystallization, the quality of the red crystals diminished and an orange powder was obtained upon evaporation of the mother liquors. Optical microscopy of this material showed two microcrystalline forms, one red and one orange, with the latter in large excess. We surmised the orange material may be the more soluble (*E*)-isomer. A portion of the orange powder was examined by X-ray powder diffraction using a PANAlytical Empyrean diffractometer operating with Cu $K\alpha_1$ radiation. It was shown to be highly crystalline, but the diffraction pattern of the orange powder did not match that calculated from the structure of the red crystals obtained (Supplementary Information Figure S1). It was possible to index the powder diffraction pattern of the orange powder using a large triclinic cell.

The volume of this cell (2506 $Å^3$) is approximately three times that of the cell found for the red crystals. It seems likely that the bulk of the orange sample contains the (*E*) isomer of **2e**, and the tripling of the volume suggests that there are three molecules in the asymmetric unit, perhaps two of one isomeric form and one of the other. Importantly, ^{1}H NMR of either the red or orange crystalline forms showed, in $CDCl_3$ solution, the same 1:1 mixture of the two geometric isomers.

We were able to select a small single crystal of the orange material from among the original red crystals. The small crystal only diffracted weakly but we were able to obtain a crystal structure, albeit of lower quality than that of the red form.[18] The structure is not too dissimilar to that of the red crystals, however it had a different orientation of both the *N*-ethyl and ethyl ester groups (Supplementary Information Figure S2). It also showed that the nitro group was not co-planar with the NH, as in the red crystals, but was inclined at an angle of 25(1) °. The crystal structure of this orange single crystal did not, however, match the powder diffraction pattern of the bulk orange material (Supplementary Information Figure S3).

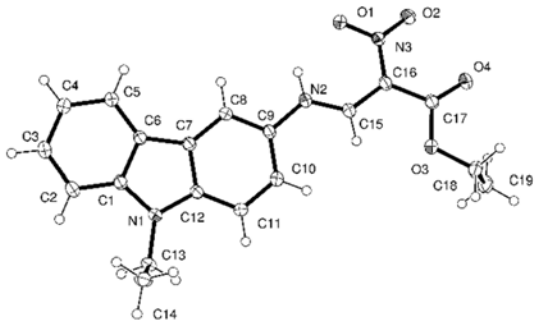

A

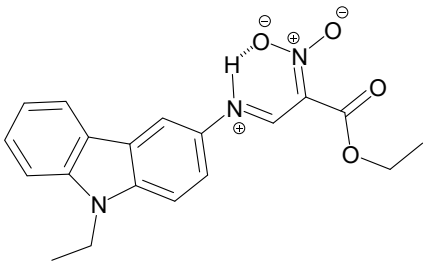

B

Figure 2A: Crystal structure of **2e** with atoms drawn as 50% thermal ellipsoids The more crystalline form of **2e** reveals a shortened N2-C15 bond, lengthened C15-C16 bond and an intermolecular hydrogen bond between the nitro group and the NH. **Figure 2B**: The bond lengths from the crystal structure of the deep red coloured **2e** is consistent with large degree of delocalisation of the nitrogen lone pair.

In order to probe the details of the interaction of these inhibitors with *Pf*DHODH, docking (with both eHiTS and Autodock) of the *E*- and *Z*-forms of **2e** and **3e** into the putative ubiquinione binding channel of *Pf*DHODH was performed using the *Pf*DHODH crystal structure (PDB code; 1TV5). The data produced suggest several possibilities for the binding of each isomer of **2e** and **3e** into *Pf*DHODH. However all of the suggested poses are predicted to bind in the same general space of the enzyme, with the aromatic 'tail' group of each ligand binding deep within the large hydrophobic pocket of the binding site (Figures 3A and 3B). For each of the four structures (i.e. both *E*- and *Z*-isomers of both **2e** and **3e**) two equally favourable rotamers were observed with the tail group seen to adopt the orientations shown in Figures 3A and 3B.

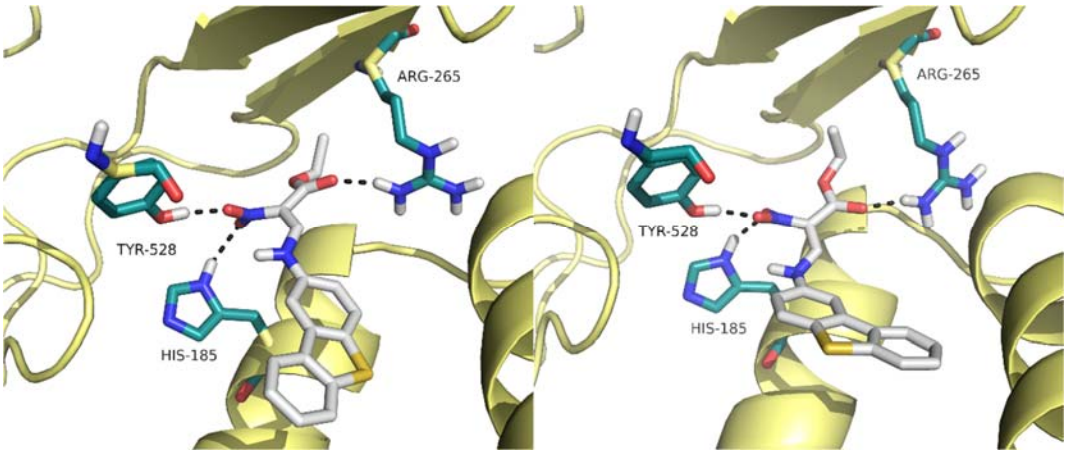

A **B**

Figure 3. Docking studies reveal that the hydrophobic aromatic tail group of **3e** (forest green) and **2e** (latter not shown) may adopt one of two equally preferred conformations (**3A** and **3B**, rotated 180° around the Ar-NH bond) when docked into the ubiquinone co-factor channel of *Pf*DHODH. In both cases hydrogen bonding networks with Tyr528, His185 and Arg265 are maintained.

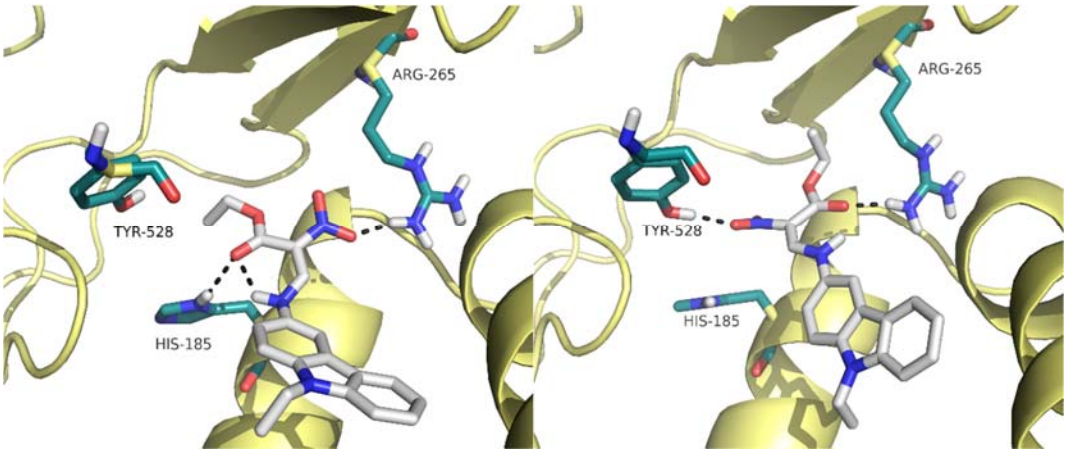

A **B**

Figure 4. Docking studies reveal that the hydrophilic head group of **2e** and **3e** (latter not shown) may bind in two equally preferred conformations (**4A** and **4B**, rotated 180° around the Ar-NH bond) when docked into the ubiquinone co-factor channel of *Pf*DHODH.

For both molecules **2e** and **3e** the polar 'head group' of the molecule is predicted to bind in the polar region of the binding site. Both isomers of each molecule can adopt two distinct hydrogen

bonding networks (Figures 4A and 4B). This is again due to a rotation of 180° around Ar-NH bond causing the polar 'head' of the molecule to flip. Although this 'flipping' forces a change in the hydrogen bonds made by the molecule and the enzyme, the residues involved in binding in *Pf*DHODH are preserved, i.e. histidine$_{185}$ (H185), tyrosine$_{528}$ (Y528) and arginine$_{265}$ (R265). All suggested binding poses have hydrogen bonds to at least two of these residues. The results from the docking studies suggest that the ligands may bind with multiple poses to the ubquinone channel and that there is no clear preference for any one arrangement.

In conclusion, we have discovered two new derivatives (**2e** and **3e**) that are potent inhibitors of *Pf*DHODH. ^{1}H and ^{13}C NMR spectroscopic data revealed that these compounds undergo ready isomerisation at room temperature in d_6-DMSO, but the docking studies indicate that there is neither conformation nor configuration which binds preferentially to *Pf*DHODH. This flexibility is favourable for inhibitors of this channel that require extensive positioning to reach their binding site. X-ray crystallographic study of the red crystal form of (*Z*)-**2e** reveals shortened N2-C15 and lengthened C15-C16 bonds. The delocalisation of the charge onto the nitro group must promote the hydrogen bonding interactions between the nitro group and the N9-H, but also with any H-bond donor group on the enzyme. This is consistent with the observations made by Phillips and co-workers where an intrinsic dipole contribution[9b] in their triazolopyrimidine class of compounds is also believed to add to the hydrogen bonding and thus binding of the inhibitors to the enzyme. Overall, these results further add to the knowledge of inhibitor binding to the co-factor binding site of *Pf*DHODH and may assist in the design and optimisation of other, more drug-like inhibitors of *P. falciparum* dihydroorotate dehydrogenase.

Acknowledgements

We thank the University of Hull for funding, BBSRC for support (GM), and the EPSRC National Mass Spectrometry Service (Swansea) for accurate mass determination of **2e** and **3e**.

References and notes

1. World Malaria Report 2016, World Health Organisation, Geneva (http://www.who.int/malaria/publications/world-malaria-report-2016/en/).
2. Schlitzer, M. *ChemMedChem* **2007**, *2*, 944–986.
3. (a) Parija, S. C.; Praharaj, I. *Indian J. Med. Microbiol.* **2011**, *29*, 243-248; (b) White, N. J. *J. Clin. Invest.* **2004**, *113*, 1084–1092.
4. (a) MMV Global portfolio of antimalarial medicines 2016, https://www.mmv.org/sites /default/files/uploads/docs/RandD/4Q_2016_Global_Portfolio.pptx (accessed 19/4/2017); (b) Arora, N.; Banerjee, A.K. *Mini-Rev. Med. Chem.* **2012**, *12*, 210-226; (c) Burrows, J. N.; Waterson, D. *Top. Med. Chem.* **2011**, *7*, 125-180; (d) Burrows, J. N.; Chibale, K.; Wells, T. N. C. *Curr. Top. Med. Chem.* **2011**, *11*, 1226-1254; (e) Schlitzer, M.; Ortmann, R. *ChemMedChem* **2010**, *5*, 1837-1840.
5. (a) McRobert, L.; McConkey, G. A. *Mol. Biochem. Parasitol.* **2002**, *119*, 273-8; (b) Phillips, M. A.; Rathod, P. K. *Infect. Dis. Drug Targ.* **2010**, *10*, 226-239.
6. (a) Boa, A. N.; Canavan, S. P.; Hirst, P. R.; Ramsey, C.; Stead, A. M. W.; McConkey, G. A. *Bioorg. Med. Chem.* **2005**, *13*, 1945-1967; (b) Hurt, D. E.; Sutton, A. E.; Clardy, J. *Bioorg. Med. Chem. Lett*. **2006**, *16*, 1610-1615.
7. (a) Baldwin, J., Michnoff, C. H.; Malmquist, N. A.; White, J.; Roth. M. G.; Rathod, P. K.; Phillips, M. A. *J. Biol. Chem.* **2005**, *280*, 21847-21853; (b) Patel, V.; Booker, M.; Kramer, M.; Ross, L.; Celatka, C. A.; Kennedy, L. M.; Dvorin, J. D.; Duraisingh, M. T.; Sliz, P.; Wirth, D. F.; Clardy, J. *J. Biol. Chem*. **2008**, *283*, 35078-35085 (c) Booker, M. L.; Bastos, C. M.; Kramer,

M. L.; Barker, R. H.; Skerlj, R.; Sidhu, A. B.; Deng, X.; Celatka, C.; Cortese, J. F.; Guerrero Bravo, J. E.; Crespo Llado, K. N.; Serrano, A. E.; Angulo-Barturen, I.; Jiménez-Díaz, M. B.; Viera, S.; Garuti, H.; Wittlin, S.; Papastogiannidis, P.; Lin, J. W.; Janse, C. J.; Khan, S. M.; Duraisingh, M.; Coleman, B.; Goldsmith, E. J.; Phillips, M. A.; Munoz, B.; Wirth, D. F.; Klinger, J. D.; Wiegand, R.; Sybertz, E. *J. Biol. Chem.* **2010**, *285*, 33054-33064.

8. (a) Heikkilä, T.; Thirumalairajan, S.; Davies, M.; Parsons, M. R.; McConkey, G. A.; Fishwick, C. W. G.; Johnson, A. P. *Bioorg. Med. Chem. Lett.* **2006**, *16*, 88-92; (b) Davies, M.; Heikkilä, T.; McConkey, G.A.; Fishwick, C. W. G.; Parsons, M. R.; Johnson, A.P. *J. Med. Chem.* **2009**, *52*, 2683-2693.

9. (a) Hurt, D. E.; Widom, J.; Clardy, J.; *Acta Crystallogr., Sect. D: Biol. Crystallogr.* **2006**, *62*, 312-23; (b) Deng, X.; Gujjar, R.; El Mazouni, F.; Kaminsky, W.; Malmquist, N. A.; Goldsmith, E. J.; Rathod, P. K.; Phillips, M. A. *J. Biol. Chem.* **2009**, *284*, 26999-27009.

10. (a) Heikkilä, T.; Ramsey, C.; Davies, M.; Galtier, C.; Stead, A. M. W.; Johnson, A. P.; Fishwick, C. W. G.; Boa, A. N.; McConkey, G. A. *J. Med. Chem.* **2007**, *50*, 186–191; (b) Cowen, D.; Bedingfield, P.; McConkey, G. A.; Fishwick, C. W. G.; Johnson, A. P. *Bioorg. Med. Chem. Lett.* **2010**, *20*, 1284–1287.

11. Fritzson, I.; Bedingfield, P. T. P.; Sundin, A. P.; McConkey, G.; Nilsson, U. J. *Med. Chem. Comm.* **2011**, *2*, 895-898.

12. (a) Coteron, J. M.; Marco, M.; Esquivias, J.; Deng, X.; White, K. L.; White, J.; Koltun, M.; El Mazouni, F.; Kokkonda, S.; Katneni, K.; Bhamidipati, R.; Shackleford, D. M.; Angulo-Barturen, I.; Ferrer, S. B.; Jiménez-Díaz, M. B.; Gamo, F. J.; Goldsmith, E. J.; Charman, W. N.; Bathurst, I.; Floyd, D.; Matthews, D.; Burrows, J. N.; Rathod, P. K.; Charman, SA.; Phillips, M. A. *J. Med. Chem.* **2011**, *54*, 5540-5561; (b) Gujjar, R.; Marwaha, A.; El Mazouni, F.; White, J.; White, K. L.; Creason, S.; Shackleford, D. M.; Baldwin, J.; Charman, W. N.; Buckner, F. S.; Charman, S.;

Rathod, P. K.; Phillips, M. A. *J. Med. Chem*. **2009**, *52*, 1864-1872; (c) Phillips, M. A.; Gujjar, R.; Malmquist, N. A.; White, J.; El Mazouni, F.; Baldwin, J.; Rathod, P. K. *J. Med. Chem.* **2008**, *51*, 3649-3653.

13. (a) Ashley, E. *Lancet Infect. Dis.* 2017, dx.doi.org/10.1016/S1473-3099(17)30172-X; (b) McCarthy, J. S.; Lotharius, J.; Rückle, T.; Chalon, S.; Phillips, M. A.; Elliott, S.; Sekuloski, S.; Griffin, P.; Ng, C. L.; Fidock, D. A.; Marquart, L.; Williams, N. S.; Gobeau, N.; Bebrevska, L.; Rosario, M.; Marsh, K.; Möhrle, J. J. *Lancet Infect. Dis.* 2017, dx.doi.org/10.1016/S1473-3099(17)30172-X; (c) Sulyok, M. ; Rückle, T.; Roth, A.; Mürbeth, R. E.; Chalon, S.; Kerr, N.; Schnieper Samec, S.; Gobeau, N.; Lamsfus Calle, C.; Ibáñez, J.; Sulyok, Z.; Held, J.; Gebru, T.; Granados, P.; Brückner, S.; Nguetse, C.; Mengue, J.; Lalremruata, A.; Sim, K. L.; Hoffman, S. L.; Möhrle, J. J.; Kremsner, P. G.; Mordmüller, B., *Lancet Infect. Dis.* 2017, http://dx.doi.org/10.1016/S1473-3099(17)30139-1.

14. Baumgartner, R.; Walloschek, M.; Kralik, M.; Gotschlich, A.; Tasler, S.; Mies, J.; Leban, J. *J. Med. Chem.* **2006**, *49*, 1239-1247.

15. *Typical experimental procedure*: Preparation of (*E*/*Z*)-ethyl 3-(9'-ethyl-9*H*-carbazol-3'-ylamino)-2-nitroacrylate (**2e**). A mixture of ethyl nitroacetate (3.99 g, 30 mmol) and triethylorthoformate (30 cm^3) in toluene (40 cm^3) was heated under reflux in a nitrogen atmosphere for 2.5 h. After cooling 3-amino-9-ethylcarbazole (5.00 g, 24 mmol) was added to this mixture, which was stirred for 10 minutes, to ensure thorough mixing, before being heated under reflux for a further period of 1 hour. The reaction mixture was then cooled and left to stand overnight. The resulting solid was collected by filtration and was washed carefully with toluene (2 × 20 cm^3). The resulting orange-red solid was recrystallised from ethanol to yield *the title compound* as bright red crystals (4.63 g, 55%). A sample suitable for X-ray diffraction analysis was prepared by recrystallisation from ethyl acetate. ^{1}H NMR ($CDCl_3$, 400 MHz) for this 1:1

mixture of geometric isomers, both chemical shifts are given when clearly resolved. δ 11.52 [11.24] (1H, bd, *J* ~14.5 [~14.7] Hz, =CH-N*H*), 9.21 [8.66] (1H, d, *J* 14.5 [14.7] Hz, =C*H*-NH), 8.12-8.09 (1H, m, ArH), 7.95 (1H, dd, *J* 8.8, 2.2 Hz ArH), 7.57-7.52 (1H, m, ArH), 7.47-7.43 (2H, m, ArH), 7.37-7.28 (2H, m, ArH), 4.45 (2H, q, *J* 7.1 Hz, OCH_2 or NCH_2), 4.42-4.36 (2H, m, NCH_2 or OCH_2), 1.48-1.43 (3H, m, CH_2CH_3), 1.41 (3H, t, *J* 7.1 Hz, CH_2CH_3); ^{13}C-NMR ($CDCl_3$, 100 MHz) δ 164.99 [161.48], 149.82 [146.00], 140.73 [140.70], 138.60 [138.37], 130.07 [129.88], 126.86 [126.77], 123.74 [123.72], 122.09 [122.06], 120.71, 119.53 [119.45], 118.28 [117.38], 117.00 [116.69], 110.60 [110.06], 109.58 [109.54], 108.99 [108.94], 61.52 [61.35], 37.79 [37.76], 14.37 [14.28], 13.78; MS (ESI) *m/z* 354.1449, $[C_{19}H_{19}N_3O_4+H]^+$ requires 354.1448. Also observed were 724.3085 ($M_2NH_4^+$, calc. 724.3089) and 1077.4459 ($M_3NH_4^+$, calc. 1077.4465); Anal. ($C_{19}H_{19}N_3O_4$) Found: C, 64.74 %; H, 6.41 %; N, 11.70 %. Calcd. C, 64.58 %; H, 5.42 %; N, 11.89 %. In a similar fashion (*E*/*Z*)-ethyl 3-(dibenzothiophen-2'-ylaminomethylene)-2-nitroacrylate (**3e**) was prepared from ethyl nitroacetate (0.45 g, 7.5 mol) and 3-aminodibenzothiophene (0.5 g, 2.5 mol) to give *the title compound* as a lemon yellow, crystalline solid (0.61 g, 71%). ^{1}H NMR ($CDCl_3$, 400 MHz) δ 11.37 [11.18] (1H, bd, *J* ~14.3 [~14.3] Hz, =CH-N*H*), 9.22 [8.68] (1H, d, *J* 14.3 [14.3] Hz, =C*H*-NH), 8.20-8.16 (1H, m, ArH), 7.99 (1H, dd, *J* 8.5, 2.4 Hz ArH), 7.93 (1H, d, *J* 8.5 Hz, ArH), 7.91-7.86 (2H, m, ArH), 7.56-7.51 (2H, m, ArH), 7.39-7.33 (1H, m, ArH), 4.46 [4.39] (2H, q, *J* 7.2 Hz, OCH_2), 1.45 [1.41] (3H, t, *J* 7.2 Hz, CH_2CH_3); ^{13}C-NMR (*d*$_6$-DMSO, 100 MHz, at 24.1 °C) 139.5, 136.6, 136.1, 136.0, 134.6, 127.6, 124.9, 123.9, 123.2, 122.4, 119.3, 112.5 (broad), 60.8, 14.2; MS (EI) *m/z* 342 (M^+), 326, 252, 235, 222, 183, 139; Anal. ($C_{17}H_{14}N_2O_4S$) Found: C, 59.48 %; H, 4.25 %; N, 8.20%. Calcd. C, 59.64 %; H, 4.12 %; N, 8.18 %.

16. Reaction of *o*-toluidine with **6a** gave a product with an NMR indicating a 1:9 ratio of doubled signals [δ 7.45 ppm vs 10.89 ppm for the NH, and δ 8.36 ppm vs 7.87 ppm for the CH]. This

however is due to the presence of rotamers about the N-Ar bond due to the *ortho* methyl group. Crystallization of this derivative is induced by cooling a hexane solution, rather than dissolution in boiling ethanol, as used for **2f** and **3f**. The heat presumably encourages any interconversion of isomers in the latter case.

17. CCDC 857094 contains the supplementary crystallographic data for the red crystalline form of (Z)-**2e** at 150 K. These data can be obtained free of charge from the Cambridge Crystallographic Data Centre, 12 Union Road, Cambridge CB2 1EZ, UK; fax: (+44) 1223-336-033; e-mail: deposit@ccdc.cam.ac.uk or via http://www.ccdc.cam.ac.uk/conts/retrieving.html.

18. CCDC 1550062 contains the supplementary crystallographic data for the orange crystalline form of **2e** at 150 K. These data can be obtained free of charge from the Cambridge Crystallographic Data Centre, 12 Union Road, Cambridge CB2 1EZ, UK; fax: (+44) 1223-336-033; e-mail: deposit@ccdc.cam.ac.uk or via http://www.ccdc.cam.ac.uk/conts/retrieving.html.

Supplementary Information

Interconvertible geometric isomers of *Plasmodium falciparum* dihydroorotate dehydrogenase inhibitors exhibit multiple binding modes

Glenn A. McConkey[a], Paul T. P. Bedingfield[a], David R. Burrell[b], Nicholas C. Chambers[b], Fraser Cunningham[c], Timothy J. Prior[b], Colin W.G. Fishwick[c], Andrew N. Boa[b*]

[a] *School of Biology, Faculty of Biological Sciences, University of Leeds, Leeds LS2 9JT, UK*

[b] *School of Mathematics & Physical Sciences,* ***Faculty of Science and Engineering,*** *University of Hull, Hull HU6 7RX, UK*

[c] *School of Chemistry, Faculty of Mathematics and Physical Sciences, University of Leeds, Leeds LS2 9JT, UK*

CCDC 857094 contains the supplementary crystallographic data for the red crystalline form of (*Z*)-**2e** at 150 K. These data can be obtained free of charge from the Cambridge Crystallographic Data Centre, 12 Union Road, Cambridge CB2 1EZ, UK; fax: (+44) 1223-336-033; e-mail: deposit@ccdc.cam.ac.uk or via http://www.ccdc.cam.ac.uk/conts/retrieving.html.

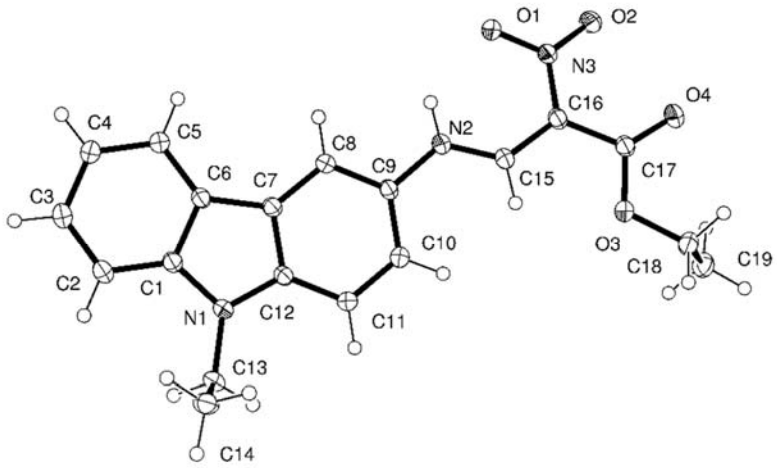

Table S1. Crystal data and structure refinement for (*Z*)-**2e** (red crystals)

Identification code	shelx	
Empirical formula	C19 H19 N3 O4	
Formula weight	353.38	
Temperature	120(2) K	
Wavelength	0.71073 Å	
Crystal system	Triclinic	
Space group	P -1	
Unit cell dimensions	a = 8.7617(18) Å	α= 87.020(16)°.
	b = 8.8742(18) Å	β= 71.107(15)°.
	c = 12.804(2) Å	γ = 61.257(14)°.
Volume	819.4(3) $Å^3$	
Z	2	
Density (calculated)	1.432 Mg/m^3	
Absorption coefficient	0.102 mm^{-1}	

F(000)	372
Crystal size	0.120 × 0.120 × 0.030 mm^3
Theta range for data collection	2.638 to 30.043°.
Index ranges	$-12 \leq h \leq 11$, $-12 \leq k \leq 10$, $-18 \leq l \leq 18$
Reflections collected	8275
Independent reflections	4779 [R(int) = 0.0513]
Completeness to theta = 25.242°	99.3 %
Refinement method	Full-matrix least-squares on F^2
Data / restraints / parameters	4779 / 0 / 237
Goodness-of-fit on F^2	1.002
Final R indices [I>2sigma(I)]	R1 = 0.0464, wR2 = 0.1215
R indices (all data)	R1 = 0.0759, wR2 = 0.1371
Extinction coefficient	none
Largest diff. peak and hole	0.270 and -0.306 $e.Å^{-3}$

Table S2. Atomic coordinates (x 10^4) and equivalent isotropic displacement parameters ($Å^2$x 10^3) for (*Z*)-**2e** (red crystals). U(eq) is defined as one third of the trace of the orthogonalized U^{ij} tensor.

	x	y	z	U(eq)
N(1)	7438(2)	6270(2)	-1928(1)	24(1)
C(1)	8896(2)	4945(2)	-2738(1)	22(1)
C(2)	8862(2)	4116(2)	-3623(1)	26(1)
C(3)	10529(2)	2771(2)	-4302(1)	28(1)
C(4)	12188(2)	2266(2)	-4112(1)	27(1)
C(5)	12237(2)	3108(2)	-3250(1)	24(1)
C(6)	10572(2)	4477(2)	-2558(1)	21(1)
C(7)	10097(2)	5634(2)	-1616(1)	21(1)
C(8)	11136(2)	5839(2)	-1063(1)	21(1)
C(9)	10213(2)	7101(2)	-153(1)	21(1)
C(10)	8273(2)	8115(2)	239(1)	24(1)
C(11)	7232(2)	7927(2)	-311(1)	24(1)
C(12)	8153(2)	6709(2)	-1251(1)	22(1)
C(13)	5534(2)	7207(2)	-1910(1)	25(1)
C(14)	5256(2)	8549(2)	-2716(1)	30(1)
N(2)	11312(2)	7266(2)	396(1)	23(1)
C(15)	10713(2)	8497(2)	1200(1)	22(1)
C(16)	11643(2)	8680(2)	1840(1)	23(1)
N(3)	13491(2)	7423(2)	1680(1)	25(1)
O(1)	14338(1)	6288(1)	846(1)	28(1)
O(2)	14255(2)	7403(2)	2341(1)	42(1)
C(17)	10680(2)	10153(2)	2731(1)	24(1)
O(3)	8879(1)	11120(1)	2822(1)	26(1)
O(4)	11362(2)	10485(2)	3297(1)	35(1)
C(18)	7786(2)	12655(2)	3641(1)	28(1)
C(19)	6932(2)	12254(2)	4761(1)	33(1)

Table S3. Bond lengths [Å] and angles [°] for (*Z*)-**2e** (red crystals).

N(1)-C(1)	1.3840(18)	C(16)-C(17)	1.4812(19)
N(1)-C(12)	1.3841(17)	N(3)-O(2)	1.2326(16)
N(1)-C(13)	1.4549(18)	N(3)-O(1)	1.2592(16)
C(1)-C(2)	1.3975(19)	C(17)-O(4)	1.2007(17)
C(1)-C(6)	1.4161(19)	C(17)-O(3)	1.3526(18)
C(2)-C(3)	1.387(2)	O(3)-C(18)	1.4547(17)
C(2)-H(2)	0.9500	C(18)-C(19)	1.501(2)
C(3)-C(4)	1.402(2)	C(18)-H(18A)	0.9900
C(3)-H(3)	0.9500	C(18)-H(18B)	0.9900
C(4)-C(5)	1.3872(19)	C(19)-H(19A)	0.9800
C(4)-H(4)	0.9500	C(19)-H(19B)	0.9800
C(5)-C(6)	1.3996(19)	C(19)-H(19C)	0.9800
C(5)-H(5)	0.9500		
C(6)-C(7)	1.4407(18)	C(1)-N(1)-C(12)	108.18(11)
C(7)-C(8)	1.3973(18)	C(1)-N(1)-C(13)	124.98(12)
C(7)-C(12)	1.4133(19)	C(12)-N(1)-C(13)	126.17(12)
C(8)-C(9)	1.3858(19)	N(1)-C(1)-C(2)	129.00(13)
C(8)-H(8)	0.9500	N(1)-C(1)-C(6)	109.36(12)
C(9)-C(10)	1.4052(19)	C(2)-C(1)-C(6)	121.63(13)
C(9)-N(2)	1.4242(17)	C(3)-C(2)-C(1)	117.54(13)
C(10)-C(11)	1.3884(19)	C(3)-C(2)-H(2)	121.2
C(10)-H(10)	0.9500	C(1)-C(2)-H(2)	121.2
C(11)-C(12)	1.3919(19)	C(2)-C(3)-C(4)	121.25(13)
C(11)-H(11)	0.9500	C(2)-C(3)-H(3)	119.4
C(13)-C(14)	1.516(2)	C(4)-C(3)-H(3)	119.4
C(13)-H(13A)	0.9900	C(5)-C(4)-C(3)	121.47(13)
C(13)-H(13B)	0.9900	C(5)-C(4)-H(4)	119.3
C(14)-H(14A)	0.9800	C(3)-C(4)-H(4)	119.3
C(14)-H(14B)	0.9800	C(4)-C(5)-C(6)	118.26(13)
C(14)-H(14C)	0.9800	C(4)-C(5)-H(5)	120.9
N(2)-C(15)	1.3201(17)	C(6)-C(5)-H(5)	120.9
N(2)-H(2A)	0.8800	C(5)-C(6)-C(1)	119.80(12)
C(15)-C(16)	1.3914(18)	C(5)-C(6)-C(7)	133.75(13)
C(15)-H(15)	0.9500	C(1)-C(6)-C(7)	106.44(12)
C(16)-N(3)	1.4071(19)	C(8)-C(7)-C(12)	120.13(12)

C(8)-C(7)-C(6)	133.43(13)	C(15)-N(2)-C(9)	125.65(12)
C(12)-C(7)-C(6)	106.44(11)	C(15)-N(2)-H(2A)	117.2
C(9)-C(8)-C(7)	118.45(12)	C(9)-N(2)-H(2A)	117.2
C(9)-C(8)-H(8)	120.8	N(2)-C(15)-C(16)	129.45(13)
C(7)-C(8)-H(8)	120.8	N(2)-C(15)-H(15)	115.3
C(8)-C(9)-C(10)	121.32(12)	C(16)-C(15)-H(15)	115.3
C(8)-C(9)-N(2)	116.99(12)	C(15)-C(16)-N(3)	120.25(12)
C(10)-C(9)-N(2)	121.63(12)	C(15)-C(16)-C(17)	120.60(13)
C(11)-C(10)-C(9)	120.51(12)	N(3)-C(16)-C(17)	119.09(12)
C(11)-C(10)-H(10)	119.7	O(2)-N(3)-O(1)	120.62(12)
C(9)-C(10)-H(10)	119.7	O(2)-N(3)-C(16)	121.59(12)
C(10)-C(11)-C(12)	118.54(13)	O(1)-N(3)-C(16)	117.78(12)
C(10)-C(11)-H(11)	120.7	O(4)-C(17)-O(3)	123.53(13)
C(12)-C(11)-H(11)	120.7	O(4)-C(17)-C(16)	126.35(14)
N(1)-C(12)-C(11)	129.48(13)	O(3)-C(17)-C(16)	110.11(12)
N(1)-C(12)-C(7)	109.51(12)	C(17)-O(3)-C(18)	115.78(11)
C(11)-C(12)-C(7)	120.94(12)	O(3)-C(18)-C(19)	111.28(13)
N(1)-C(13)-C(14)	112.21(13)	O(3)-C(18)-H(18A)	109.4
N(1)-C(13)-H(13A)	109.2	C(19)-C(18)-H(18A)	109.4
C(14)-C(13)-H(13A)	109.2	O(3)-C(18)-H(18B)	109.4
N(1)-C(13)-H(13B)	109.2	C(19)-C(18)-H(18B)	109.4
C(14)-C(13)-H(13B)	109.2	H(18A)-C(18)-H(18B)	108.0
H(13A)-C(13)-H(13B)	107.9	C(18)-C(19)-H(19A)	109.5
C(13)-C(14)-H(14A)	109.5	C(18)-C(19)-H(19B)	109.5
C(13)-C(14)-H(14B)	109.5	H(19A)-C(19)-H(19B)	109.5
H(14A)-C(14)-H(14B)	109.5	C(18)-C(19)-H(19C)	109.5
C(13)-C(14)-H(14C)	109.5	H(19A)-C(19)-H(19C)	109.5
H(14A)-C(14)-H(14C)	109.5	H(19B)-C(19)-H(19C)	109.5
H(14B)-C(14)-H(14C)	109.5		

Symmetry transformations used to generate equivalent atoms:

Table S4. Anisotropic displacement parameters ($Å^2$x 10^3) for (*Z*)-**2e** (red crystals). The anisotropic displacement factor exponent takes the form: $-2\pi^2[h^2a^{*2}U^{11} + ... + 2 h k a^* b^* U^{12}]$

	U^{11}	U^{22}	U^{33}	U^{23}	U^{13}	U^{12}
N(1)	20(1)	26(1)	26(1)	0(1)	-11(1)	-10(1)
C(1)	23(1)	23(1)	23(1)	3(1)	-10(1)	-12(1)
C(2)	29(1)	29(1)	27(1)	4(1)	-14(1)	-16(1)
C(3)	33(1)	29(1)	25(1)	1(1)	-12(1)	-17(1)
C(4)	27(1)	26(1)	25(1)	-2(1)	-7(1)	-12(1)
C(5)	22(1)	25(1)	23(1)	0(1)	-7(1)	-11(1)
C(6)	22(1)	23(1)	22(1)	2(1)	-9(1)	-13(1)
C(7)	21(1)	22(1)	21(1)	3(1)	-8(1)	-11(1)
C(8)	20(1)	22(1)	22(1)	2(1)	-8(1)	-10(1)
C(9)	23(1)	23(1)	21(1)	2(1)	-10(1)	-12(1)
C(10)	23(1)	23(1)	24(1)	-1(1)	-8(1)	-10(1)
C(11)	19(1)	23(1)	27(1)	-1(1)	-8(1)	-8(1)
C(12)	21(1)	23(1)	23(1)	3(1)	-10(1)	-11(1)
C(13)	21(1)	30(1)	29(1)	2(1)	-12(1)	-13(1)
C(14)	23(1)	34(1)	31(1)	5(1)	-12(1)	-12(1)
N(2)	22(1)	25(1)	22(1)	1(1)	-8(1)	-12(1)
C(15)	24(1)	24(1)	22(1)	2(1)	-9(1)	-13(1)
C(16)	23(1)	27(1)	22(1)	1(1)	-8(1)	-14(1)
N(3)	22(1)	31(1)	23(1)	-1(1)	-8(1)	-14(1)
O(1)	23(1)	31(1)	28(1)	-6(1)	-7(1)	-11(1)
O(2)	27(1)	54(1)	39(1)	-13(1)	-18(1)	-10(1)
C(17)	24(1)	29(1)	22(1)	1(1)	-7(1)	-15(1)
O(3)	25(1)	28(1)	26(1)	-4(1)	-8(1)	-12(1)
O(4)	31(1)	42(1)	33(1)	-9(1)	-12(1)	-18(1)
C(18)	29(1)	25(1)	27(1)	-2(1)	-8(1)	-11(1)
C(19)	34(1)	36(1)	29(1)	-2(1)	-5(1)	-20(1)

Table S5. Hydrogen coordinates (x 10^4) and isotropic displacement parameters ($Å^2$x 10^3) for (*Z*)-**2e** (red crystals).

	x	y	z	U(eq)
H(2)	7739	4461	-3754	31
H(3)	10547	2181	-4907	33
H(4)	13304	1325	-4583	32
H(5)	13370	2765	-3133	28
H(8)	12444	5131	-1306	25
H(10)	7668	8934	885	29
H(11)	5921	8616	-51	29
H(13A)	4702	7788	-1148	30
H(13B)	5193	6373	-2104	30
H(14A)	6101	7983	-3469	45
H(14B)	5512	9422	-2497	45
H(14C)	3974	9109	-2702	45
H(2A)	12493	6480	181	34
H(15)	9464	9389	1365	27
H(18A)	6795	13559	3392	34
H(18B)	8588	13116	3699	34
H(19A)	7913	11433	5037	50
H(19B)	6188	11743	4697	50
H(19C)	6138	13324	5282	50

CCDC 1550062 contains the supplementary crystallographic data for the orange crystalline form of **2e** at 150 K. These data can be obtained free of charge from the Cambridge Crystallographic Data Centre, 12 Union Road, Cambridge CB2 1EZ, UK; fax: (+44) 1223-336-033; e-mail: deposit@ccdc.cam.ac.uk or via http://www.ccdc.cam.ac.uk/conts/retrieving.html.

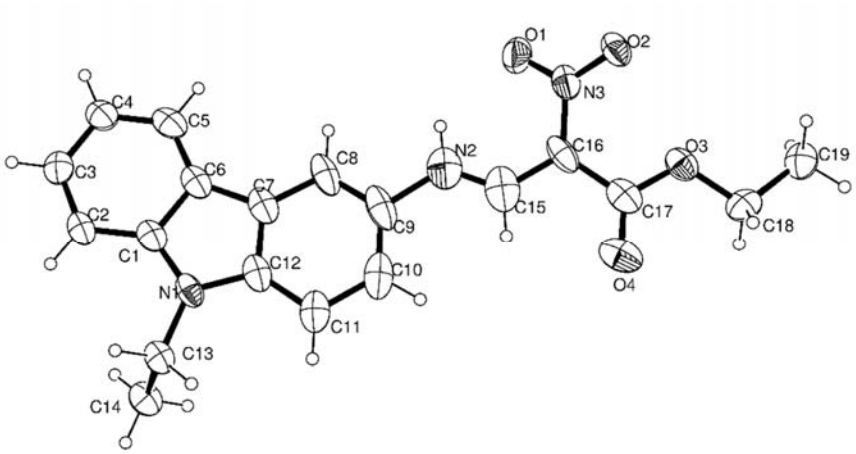

Table S6. Crystal data and structure refinement for **2e** (orange crystal).

Identification code	shelx	
Empirical formula	C19 H19 N3 O4	
Formula weight	353.37	
Temperature	150(2) K	
Wavelength	0.71073 Å	
Crystal system	Triclinic	
Space group	P -1	
Unit cell dimensions	a = 8.123(2) Å	α= 91.517(16)°.
	b = 8.2709(17) Å	β= 102.586(18)°.
	c = 13.834(3) Å	γ = 110.110(18)°.
Volume	846.6(3) $Å^3$	
Z	2	
Density (calculated)	1.386 Mg/m^3	

Absorption coefficient	0.099 mm^{-1}
F(000)	372
Crystal size	0.230 × 0.140 × 0.030 mm^3
Theta range for data collection	2.639 to 25.701°.
Index ranges	$-9 \leq h \leq 9$, $-10 \leq k \leq 9$, $-16 \leq l \leq 16$
Reflections collected	7363
Independent reflections	3202 [R(int) = 0.1891]
Completeness to theta = 25.242°	99.9 %
Refinement method	Full-matrix least-squares on F^2
Data / restraints / parameters	3202 / 0 / 235
Goodness-of-fit on F^2	1.020
Final R indices [I>2sigma(I)]	R1 = 0.1037, wR2 = 0.2756
R indices (all data)	R1 = 0.2014, wR2 = 0.3482
Extinction coefficient	none
Largest diff. peak and hole	1.169 and -0.357 $e.Å^{-3}$

Table S7. Atomic coordinates (x 10^4) and equivalent isotropic displacement parameters ($Å^2$x 10^3) for **2e** (orange crystal). U(eq) is defined as one third of the trace of the orthogonalized U^{ij} tensor.

	x	y	z	U(eq)
C(1)	4044(9)	3717(7)	8594(4)	60(2)
C(2)	3184(9)	3231(8)	9377(4)	60(2)
C(3)	1912(10)	3928(8)	9483(5)	66(2)
C(4)	1465(10)	5088(8)	8850(5)	69(2)
C(5)	2313(11)	5554(8)	8088(5)	71(2)
C(6)	3625(10)	4912(7)	7950(4)	63(2)
C(7)	4804(10)	5180(8)	7279(4)	68(2)
C(8)	5062(12)	6246(8)	6525(5)	80(2)
C(9)	6317(13)	6298(9)	6041(5)	88(3)
C(10)	7348(11)	5213(10)	6243(5)	87(3)
C(11)	7137(10)	4070(9)	7010(5)	77(2)
C(12)	5845(9)	4104(8)	7528(4)	65(2)
C(13)	6129(9)	2028(7)	8823(4)	60(2)
C(14)	4969(9)	156(8)	8461(5)	70(2)
C(15)	7619(12)	7819(11)	4745(6)	92(3)
C(16)	8059(10)	9077(8)	4119(5)	71(2)
C(17)	9406(10)	8984(8)	3578(5)	69(2)
C(18)	10848(10)	9885(9)	2286(5)	72(2)
C(19)	10808(10)	11087(9)	1503(5)	76(2)
N(1)	5383(7)	3255(6)	8321(3)	60(1)
N(2)	6573(10)	7578(8)	5295(5)	89(2)
N(3)	7390(9)	10469(7)	4063(4)	68(2)
O(1)	5949(9)	10215(6)	4311(4)	95(2)
O(2)	8247(6)	11864(5)	3796(3)	70(1)
O(3)	9595(6)	10009(5)	2866(3)	67(1)
O(4)	10210(8)	7986(6)	3765(4)	89(2)

Table S8. Bond lengths [Å] and angles [°] for **2e** (orange crystal).

C(1)-N(1)	1.388(9)	C(16)-C(17)	1.474(11)
C(1)-C(2)	1.409(9)	C(17)-O(4)	1.218(8)
C(1)-C(6)	1.426(9)	C(17)-O(3)	1.316(8)
C(2)-C(3)	1.375(10)	C(18)-O(3)	1.454(8)
C(2)-H(2)	0.9500	C(18)-C(19)	1.492(10)
C(3)-C(4)	1.402(9)	C(18)-H(18A)	0.9900
C(3)-H(3)	0.9500	C(18)-H(18B)	0.9900
C(4)-C(5)	1.375(10)	C(19)-H(19A)	0.9800
C(4)-H(4)	0.9500	C(19)-H(19B)	0.9800
C(5)-C(6)	1.388(10)	C(19)-H(19C)	0.9800
C(5)-H(5)	0.9500	N(2)-H(2A)	0.8800
C(6)-C(7)	1.442(10)	N(3)-O(2)	1.239(6)
C(7)-C(8)	1.388(9)	N(3)-O(1)	1.242(8)
C(7)-C(12)	1.426(10)		
C(8)-C(9)	1.326(12)	N(1)-C(1)-C(2)	130.3(6)
C(8)-H(8)	0.9500	N(1)-C(1)-C(6)	108.9(6)
C(9)-C(10)	1.419(13)	C(2)-C(1)-C(6)	120.8(7)
C(9)-N(2)	1.493(10)	C(3)-C(2)-C(1)	117.6(6)
C(10)-C(11)	1.439(11)	C(3)-C(2)-H(2)	121.2
C(10)-H(10)	0.9500	C(1)-C(2)-H(2)	121.2
C(11)-C(12)	1.401(10)	C(2)-C(3)-C(4)	122.5(6)
C(11)-H(11)	0.9500	C(2)-C(3)-H(3)	118.7
C(12)-N(1)	1.370(8)	C(4)-C(3)-H(3)	118.7
C(13)-N(1)	1.468(8)	C(5)-C(4)-C(3)	119.5(7)
C(13)-C(14)	1.512(8)	C(5)-C(4)-H(4)	120.3
C(13)-H(13A)	0.9900	C(3)-C(4)-H(4)	120.3
C(13)-H(13B)	0.9900	C(4)-C(5)-C(6)	120.7(6)
C(14)-H(14A)	0.9800	C(4)-C(5)-H(5)	119.6
C(14)-H(14B)	0.9800	C(6)-C(5)-H(5)	119.6
C(14)-H(14C)	0.9800	C(5)-C(6)-C(1)	118.9(6)
C(15)-N(2)	1.229(10)	C(5)-C(6)-C(7)	135.0(6)
C(15)-C(16)	1.374(10)	C(1)-C(6)-C(7)	106.0(6)
C(15)-H(15)	0.9500	C(8)-C(7)-C(12)	120.9(7)
C(16)-N(3)	1.430(9)	C(8)-C(7)-C(6)	132.3(8)

C(12)-C(7)-C(6)	106.8(5)	O(3)-C(17)-C(16)	114.3(6)
C(9)-C(8)-C(7)	119.9(8)	O(3)-C(18)-C(19)	107.1(6)
C(9)-C(8)-H(8)	120.1	O(3)-C(18)-H(18A)	110.3
C(7)-C(8)-H(8)	120.1	C(19)-C(18)-H(18A)	110.3
C(8)-C(9)-C(10)	121.2(7)	O(3)-C(18)-H(18B)	110.3
C(8)-C(9)-N(2)	115.6(9)	C(19)-C(18)-H(18B)	110.3
C(10)-C(9)-N(2)	123.2(9)	H(18A)-C(18)-H(18B)	108.5
C(9)-C(10)-C(11)	121.6(8)	C(18)-C(19)-H(19A)	109.5
C(9)-C(10)-H(10)	119.2	C(18)-C(19)-H(19B)	109.5
C(11)-C(10)-H(10)	119.2	H(19A)-C(19)-H(19B)	109.5
C(12)-C(11)-C(10)	115.3(8)	C(18)-C(19)-H(19C)	109.5
C(12)-C(11)-H(11)	122.3	H(19A)-C(19)-H(19C)	109.5
C(10)-C(11)-H(11)	122.3	H(19B)-C(19)-H(19C)	109.5
N(1)-C(12)-C(11)	130.0(7)	C(12)-N(1)-C(1)	109.3(5)
N(1)-C(12)-C(7)	108.9(6)	C(12)-N(1)-C(13)	127.2(6)
C(11)-C(12)-C(7)	121.0(6)	C(1)-N(1)-C(13)	123.5(5)
N(1)-C(13)-C(14)	113.1(5)	C(15)-N(2)-C(9)	126.9(9)
N(1)-C(13)-H(13A)	109.0	C(15)-N(2)-H(2A)	116.6
C(14)-C(13)-H(13A)	109.0	C(9)-N(2)-H(2A)	116.6
N(1)-C(13)-H(13B)	109.0	O(2)-N(3)-O(1)	122.6(6)
C(14)-C(13)-H(13B)	109.0	O(2)-N(3)-C(16)	120.5(6)
H(13A)-C(13)-H(13B)	107.8	O(1)-N(3)-C(16)	116.9(6)
C(13)-C(14)-H(14A)	109.5	C(17)-O(3)-C(18)	115.7(6)
C(13)-C(14)-H(14B)	109.5		
H(14A)-C(14)-H(14B)	109.5		
C(13)-C(14)-H(14C)	109.5		
H(14A)-C(14)-H(14C)	109.5		
H(14B)-C(14)-H(14C)	109.5		
N(2)-C(15)-C(16)	130.0(10)		
N(2)-C(15)-H(15)	115.0		
C(16)-C(15)-H(15)	115.0		
C(15)-C(16)-N(3)	122.5(8)		
C(15)-C(16)-C(17)	115.2(8)		
N(3)-C(16)-C(17)	122.1(6)		
O(4)-C(17)-O(3)	124.0(8)		
O(4)-C(17)-C(16)	121.6(6)		

Symmetry transformations used to generate equivalent atoms:

Table S9. Anisotropic displacement parameters ($Å^2 x\ 10^3$)for **2e** (orange crystal). The anisotropic displacement factor exponent takes the form: $-2\pi^2[\ h^2a^{*2}U^{11} + ... + 2\ h\ k\ a^*\ b^*\ U^{12}\ ]$

	U^{11}	U^{22}	U^{33}	U^{23}	U^{13}	U^{12}
C(1)	70(4)	39(3)	52(3)	-1(3)	5(3)	2(3)
C(2)	70(4)	48(3)	46(3)	5(3)	6(3)	4(3)
C(3)	72(4)	55(3)	57(3)	-4(3)	15(3)	8(3)
C(4)	88(5)	53(3)	57(4)	-3(3)	7(4)	22(3)
C(5)	93(5)	40(3)	58(4)	-6(3)	-6(4)	13(3)
C(6)	80(5)	37(3)	46(3)	-3(2)	-1(3)	0(3)
C(7)	86(5)	43(3)	45(3)	-4(3)	1(3)	-4(3)
C(8)	104(6)	44(3)	48(3)	2(3)	6(4)	-20(3)
C(9)	112(7)	53(4)	52(4)	5(3)	5(4)	-19(4)
C(10)	83(5)	79(5)	59(4)	-15(4)	23(4)	-23(4)
C(11)	76(5)	72(4)	54(4)	-8(3)	15(3)	-6(3)
C(12)	70(4)	49(3)	48(3)	-1(3)	6(3)	-7(3)
C(13)	62(4)	51(3)	54(3)	5(3)	6(3)	10(3)
C(14)	66(4)	51(3)	74(4)	5(3)	6(3)	5(3)
C(15)	91(6)	78(5)	61(4)	-17(4)	4(4)	-16(4)
C(16)	95(5)	42(3)	46(3)	8(3)	-3(3)	-2(3)
C(17)	78(5)	46(3)	56(4)	-7(3)	-6(3)	3(3)
C(18)	72(5)	61(4)	72(4)	-18(3)	12(4)	17(3)
C(19)	79(5)	77(4)	63(4)	-6(4)	18(4)	15(4)
N(1)	69(3)	45(2)	49(3)	10(2)	7(2)	3(2)
N(2)	90(5)	74(4)	72(4)	-13(3)	12(4)	-4(3)
N(3)	88(4)	49(3)	52(3)	-2(2)	20(3)	4(3)
O(1)	116(5)	67(3)	108(4)	8(3)	68(4)	17(3)
O(2)	85(3)	48(2)	64(3)	11(2)	20(2)	8(2)
O(3)	75(3)	49(2)	61(2)	3(2)	6(2)	10(2)
O(4)	110(4)	62(3)	74(3)	-5(2)	-13(3)	28(3)

Table S10. Hydrogen coordinates (x 10^4) and isotropic displacement parameters ($Å^2$x 10^3) for **2e** (orange crystal).

	x	y	z	U(eq)
H(2)	3471	2450	9816	72
H(3)	1314	3610	10006	79
H(4)	583	5548	8947	83
H(5)	1998	6325	7651	85
H(8)	4341	6938	6356	96
H(10)	8199	5242	5862	104
H(11)	7825	3344	7154	92
H(13A)	6259	2227	9549	72
H(13B)	7349	2255	8712	72
H(14A)	5530	-601	8821	105
H(14B)	3767	-87	8583	105
H(14C)	4857	-59	7746	105
H(15)	8216	7011	4756	110
H(18A)	10478	8683	1975	86
H(18B)	12083	10222	2719	86
H(19A)	11640	11040	1095	114
H(19B)	9580	10740	1079	114
H(19C)	11177	12272	1821	114
H(2A)	5905	8228	5242	107

A portion of the orange powder, obtained from the mother liquors of the crystallisation of red (*Z*)-**2e**, was examined by X-ray powder diffraction using a PANAlytical Empyrean diffractometer operating with Cu $K\alpha_1$ radiation. The powder was shown to be highly crystalline, but the diffraction pattern of the orange powder did not match that calculated from the structure of the red crystals (Figure S2) or orange crystals obtained (Figure S3). It was possible to index the powder diffraction pattern of the orange powder using a large triclinic cell with parameters shown below. The volume of this cell (2506 $Å^3$) is approximately three times that of the cell found for the red crystals. It seems reasonable that the orange sample contains (*E*)-**2e** and the tripling of the volume suggests that there are three molecules in the asymmetric unit, perhaps two of one isomeric form and one of the other.

a = 15.93(3) Å
b = 15.03(3) Å
c = 13.07(3) Å
α = 70.08(17) °
β = 106.64(14) °
γ = 120.70(16) °

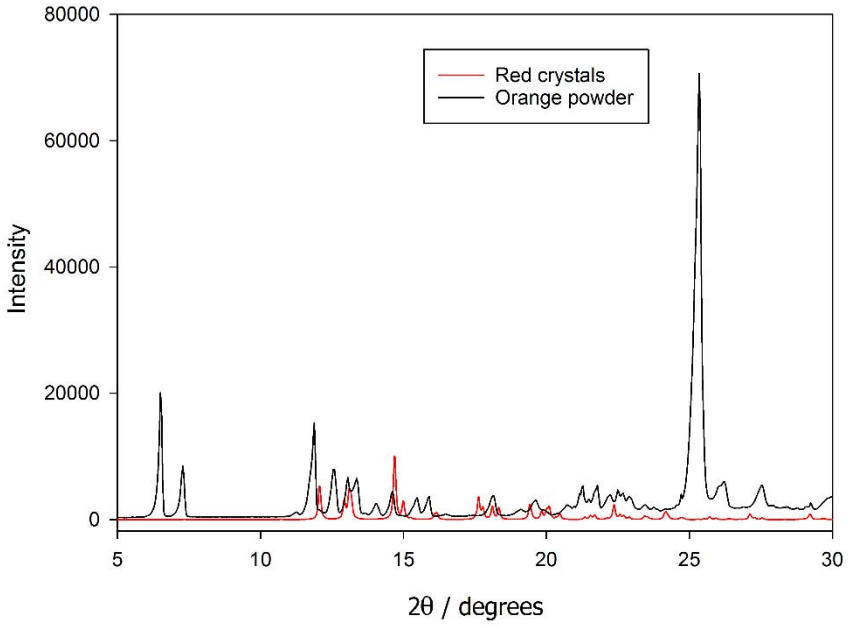

Figure S1: Powder X-ray diffraction pattern of the orange powder of **2e**, and calculated pattern of the red crystals of **2e**.

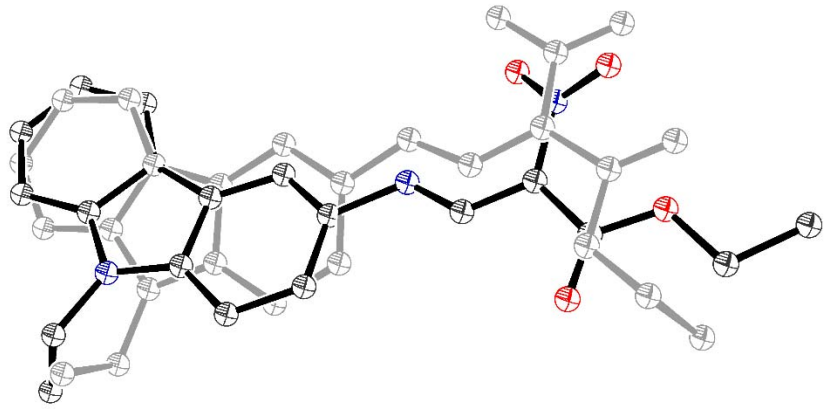

Figure S2: Overlay of the structures of the red and orange crystalline forms of **2e**.

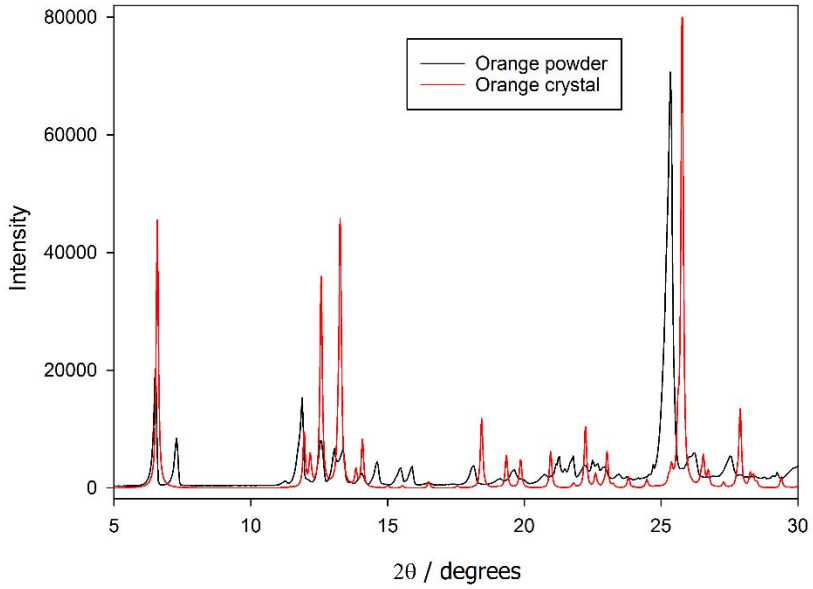

Figure S3: Powder X-ray diffraction pattern of the orange powder of **2e**, and calculated pattern of the orange crystals of **2e**.